様　式　Ｃ－１９、Ｆ－１９－１、Ｚ－１９　（共通）

科学研究費助成事業　　研究成果報告書

平成　２９　年　　６　月　１１　日現在

機関番号：　１２１０２
研究種目：　若手研究(B)
研究期間：　2015～2016
課題番号：　１５Ｋ２０８８７

研究課題名（和文）H igh-speed　optical　im aging　engine　for　m ultifunctional　investigation of the　eye

研究課題名（英文）High-speed optical imaging engine for multifunctional investigation of the ey

研究代表者

洪　暎周（Hong, Young-Joo）

筑波大学・医学医療系・助教

研究者番号：４０７３８４３１

交付決定額（研究期間全体）：（直接経費）　　2,300,000円

研究成果の概要（和文）：モーションアーチファクト（MA)の低減を目指した高速光OCTエンジンの根本的な目標を満たすための研究アプローチを変更した。それは、特に設計された走査プロトコルを用いてMAを補正することである。
リサージュ走査パターンは、頻繁に重なる軌跡を持ち、OCTスキャン用に設計され、3次元の眼球運動補正法が開発され、ソフトウェアによって自動的に修正された。動き補正なしで画像を比較することにより、この方法の有効性が示された。実験を行い、我々の方法で修正した結果を地上の真理と比較して、その妥当性を検証した。実験結果は、本手法が眼のMAを効果的に補正することを示した。さらに、我々の方法の十分な再現性が確認された。

研究成果の概要（英文）：I had replaced the research approach to meet the fundamental goal of high speed optical coherence tomography(OCT) engine which aiming reduction of motion artifacts. The another approach is the correction of motion artifacts by using particularly designed scanning protocol.
A Lissajous scanning pattern, which has a trajectory that frequently overlaps with itself, was adopted and designed for OCT volume scan, and a three-dimensional eye motion correction method was developed. Eye motion artifacts were corrected automatically by software. By comparing the image without and with the motion correction, it was shown the effectiveness of the method. An experiment was performed and the results corrected by our method was compared with the ground truths to verify its validity. The experimental results showed that our method effectively corrects eye motion artifacts. Furthermore, the sufficient repeatability of our method was confirmed.

研究分野：　Optical coherence tomography

キーワード：　OCT　motion correction　Lissajous scan

１．研究開始当初の背景

OCT provides a means to diagnose and study various ocular diseases by providing high resolution cross-sectional images non-invasively[1]. Owing to the increase of OCT measurement speed, 3D volumetric OCT imaging is also available in several seconds. However, in the case of 3D OCT imaging, the involuntary eye motion causes distortion and discontinuity of image, hence the eye motion correction is challenging issue for 3D ophthalmic imaging. One approach is based on the hardware extension to track the eye motion. Scanning laser ophthalmoscope (SLO) was combined with OCT, and the galvanometric scanning mirrors of OCT are driven to compensate the eye motion in real time[2]. It successfully corrects slow drift of lateral eye motion and does rescan for saccadic eye motion. However, it still requires axial motion correction in post-processing and it is hard to retrieve true shape. And the hardware-extension increases the expense and the complexity of the system. Another approach is to scan a volume multiple times and correct the eye motion in post-processing. The common scan pattern is to scan a volume multiple times with two orthogonal fast raster scan axes[3-5]. However, it requires multiple volume measurements and has difficulty of high speed imaging due to the high order harmonics of the raster scan frequency.

２．研究の目的

We present another eye motion correction algorithm for 3D OCT imaging of the human retina based on Lissajous scan. The Lissajous scan pattern is obtained by operating two axes with sinusoidal waveforms of different frequencies, hence this approach has potential for high-speed scan with a mechanical scanner. The scanning trajectory and velocity change of Lissajous scan pattern are smooth and continuous, hence there is no galvanometric scanning mirror pullback and no dead-time of acquisition. And any single round-trip scan trajectory crosses other scan trajectories, hence any scan trajectory can be reference for motion correction of other scan trajectories. In those reasons, we implemented eye motion correction for 3D OCT imaging based on the Lissajous scan.

３．研究の方法

3.1 Scan pattern

Our scanning pattern is based on a closed-loop Lissajous scan design originally demonstrated by Bazaei *et al.*[6]. Basic Lissajous scan waveforms for horizontal (x) and vertical (y) axes can be given as $x(t) = A_x\cos(2\pi f_x t)$ and $y(t)=A_y\cos(2\pi f_y t)$. f_x and f_y are scan frequencies of x- and y- galvanometric scanners, and have relation of $f = 1/T = |f_x - f_y|$, where f is fundamental frequency given by full single Lissajous scan time T. And the scanning frequencies of x and y axes are defined as $f_x = 2 \cdot N \cdot f$ and $f_y = (2N-1) \cdot f$, where N is a parameter determining density of scan trajectory.

In order to form Lissajous scan waveform for 3D OCT imaging, following parameters need to be defined. We defined the number of A-lines per single cycle of x-axis scan as $\#A$, and the number of cycle of x-axis scan per volume as $\#B$. The fundamental frequency is determined as $f = f_A/(\#A \cdot \#B)$, where f_A is an A-line rate of system. In the condition of $A_x = A_y$, to have equivalent distance between A-lines along and across scan trajectory, #B is determined as $\#A/2$ and N is determined as $\#B/2$. Hence by selecting #A and transversal scanning range (A_x and A_y), Lissajous scan pattern for OCT volume measurement is determined as follows.

$$x(t_i) = A_x\cos[\, 2\pi \cdot f_A \cdot t_i / \#A \,],$$

$$y(t_i) = A_y\cos[\, (2 \cdot \#A - 4)\pi \cdot f_A \cdot t_i / \#A^2 \,] \qquad (1)$$

where, t_i is the acquisition time point of i-th A-line, and the total number of A-lines in a volume is $\#A^2/2$.

Figure 1 shows an example of closed Lissajous scan pattern generated with Eq. (1). The circles on the Lissajous scan trajectory represent A-line sampling points, small A-line number per horizontal cycle (#A =64) was used for the visualization. The yellow curve indicates one of single horizontal cycles. While each single horizontal cycle changes its scan trajectory continuously, the scan trajectory crosses full range of x- and y-axes, hence any scan trajectory cross-over other scan trajectories of horizontal cycle. Within a certain short time, we can regard the OCT image is motion free. We set #A to be acquired in 10 ms with1024 A-lines for measurement, and the OCT image of horizontal cycle was regarded as motion free. And they were utilized as references for motion correction of other OCT images of horizontal cycle.

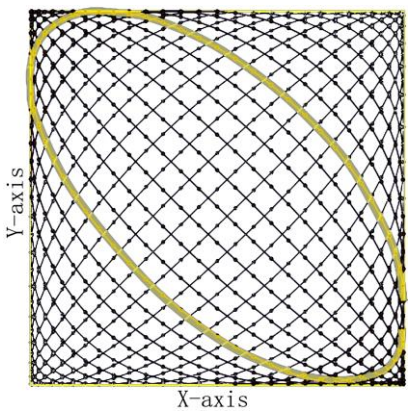

Figure 1. Characteristic of Lissajous scan. The example of Lissajous scan pattern was generated by Eq.(1) with A_x=A_y and #A=64. The circles on the scan trajectory represent A-line sampling points. The yellow curve represents one of single horizontal cycles.

3.2 Motion correction algorithm

The main idea of the motion correction algorithm is to divide the OCT measurement data to smaller parts which are regarded as motion-free. Owing to the property of Lissajous scan, each part always has laterally overlapping region with other part, and we can gradually register the small parts one by one to correct motion. However, if we use a single horizontal cycle for motion correction, motion estimation accuracy might be low in the beginning of registration, because we do not have reference for registration and the overlapped region is small. Hence, we took two step approaches for motion correction. The first step is rough correction with rather larger number of A-lines to secure certain number of overlapped region. The second step is fine correction with rather smaller number of A-lines and the final image of the rough registration can be used as reference. And that approach was taken for both of lateral and axial motion correction. The flow of the motion correction algorithm is shown in Figure 2. Because the depth profile of A-line is fundamental unit of 3D volumetric OCT image, lateral motion correction of A-lines was done first and axial shift of A-line depth profile was corrected.

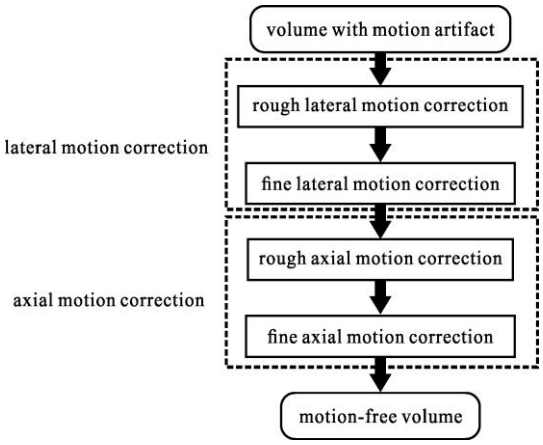

Figure 2. Motion correction processing flow.

3.2.1 Lateral motion correction algorithm

Figure 3 shows the lateral motion correction flow. First, quick lateral eye motion was detected by using the correlation coefficient between linear intensity projections of adjacent single cycles of x-axis scan. When the first order differential of the correlation coefficient is less than a threshold which was empirically determined as negative standard deviation of the first order differentials, it was regarded as moment of quick eye motion. And A-lines of measured volume were grouped into sub-volume by using the moments of quick motion as fiducial points. The sub-volume is further split into smaller sub-volume so that the maximum acquisition time of the sub-volume becomes 0.2 seconds. Then each *en face* projection of sub-volume was remapped to the grid coordinate from the actually scanned positions, and the largest sub-volume on the grid coordinate was set as a reference for the rough lateral motion correction. The lateral shifts among the sub-volumes are detected by image correlation of en face projections of the sub-volumes, where we utilized specially designed algorithm to compute the correlation between images with different and arbitrarily-shaped region of interests. The lateral shifts of each sub-volume are then corrected by using the detected motion.

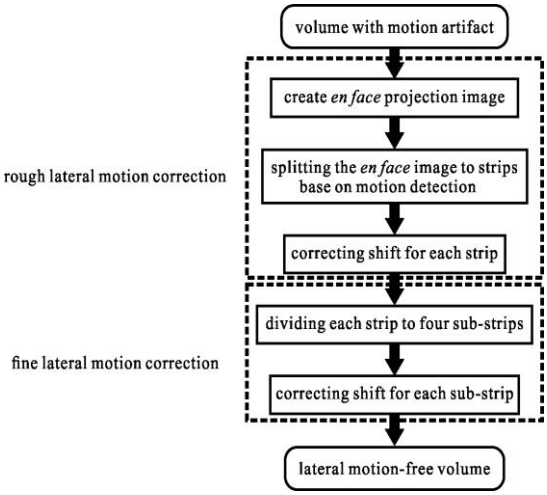

Figure 3. The flowchart of the lateral motion correction algorithm

For the fine lateral motion correction, global reference image was obtained by remapping full A-lines based on the rough lateral motion corrected scan trajectories, and each strip was divided into four sub-strips based on location. For the local four sub-strips, A-lines of any single horizontal cycle of strips divided into four time-bands, and the A-lines included in the same time-band were grouped. And the lateral shift of each local sub-strip was corrected over the global reference by using the same image correlation which was used for the rough lateral motion correction. After we correct lateral shift of all sub-strips, the global reference image was updated by remapping with full A-lines corrected by fine lateral shift correction. The global reference update and fine lateral motion correction were iterated three times.

3.2.2 Axial motion correction

Figure 4 shows the axial motion correction processing flow. First, the lateral motion-free volume was split to sub-volumes to have a fixed number of A-lines. The axial shift among sub-volumes was corrected by using depth-oriented correlation-based algorithm, where the correlation is computed for A-line pairs assigned at same grid location. The first sub-volume was set as reference and the target sub-volume, which overlaps with the reference more than one-fourth of A-lines of sub-volume, was corrected. After correcting axial shift of target sub-volume, the reference volume was updated by merging with the target sub-volume.

After the rough axial motion correction was finished, sub-volume was divided to four parts, and each one-fourth sub-volume was corrected to the reference volume. For this fine axial motion correction, the reference volume regenerated by removing the corresponding sub-volume. After the fine axial motion correction, axial shift cancelled sub-volumes were merged to build motion free 3D OCT images.

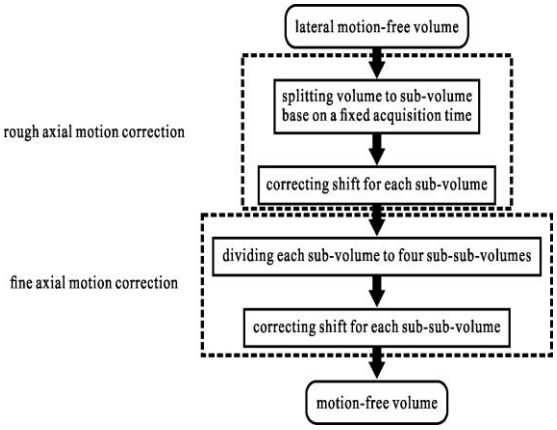

Figure 4. The flowchart of the axial motion correction algorithm.

４．研究成果

The Lissajous scan is implemented for the posterior eye with the 1-μm band Jones matrix based polarization-sensitive swept-source OCT (JM-OCT), and it has an A-line rate of 100 kHz and probing power is 1.4mW. The transversal area of 6mm × 6mm is scanned by Lissajous scan with #A=1024, and it takes 5.2 seconds for single volume measurement. In this paper, the coherent composited intensity of 4 entries of Jones matrix tomography, which has similar property with standard scattering OCT, was utilized for motion correction.

Figure 5 shows images of optic nerve head (ONH) region scanned with (a, b) Lissajous and (c) raster scan. The total number of A-lines of raster scan is same with that of Lissajous scan as 512 × 1024, however the measurement time was 6.6 seconds, due to the galvanometric mirror scanner pullback. Columns of Figs. 5(a) – 5(c) show remapped Lissajous scan images without and with eye motion correction and raster scan image, respectively. Rows of Figs. 5(1) – (3) show *en face* projection, horizontal cross-section and vertical cross-section images. The effectiveness of motion correction is clear by comparing Lissajous scanned images (b) with and (a) without motion correction, *en face* projection image shows rather clear vasculature and cross-section images show rather clear layered structure due to the proper lateral and axial motion correction.

Comparison with raster scanned image [Fig. 5(c)] might be straightforward to understand the advantage of Lissajous can. The horizontal line artifacts on the *en face* projection image of raster scan were caused by eye motion [Fig. 5(c1)]. The fast scan oriented cross-sectional image of raster scan may provide the true shape of the posterior eye [Fig. 5(c2)], and we can find the horizontal cross-section of Lissajous [Fig. 5(b2)] show similar shape, even the horizontal cross-section was composed with discontinuous A-lines. In the case of the slow-scan oriented cross-sectional image [Fig. 5(c3)], it is hard to obtain true shape cross-section, even we apply axial shift correction, because we correct axial shift along slow scan direction by comparing non-overlapped adjacent cross-section images. On the other hand, the cross-sectional images obtained by Lissajous scan and motion correction provide true shape of posterior eye. The curvature of retinal pigment epithelium (RPE) layer of the vertical cross-sectional image [Fig. 5(b3)] is clear evidence, while it is hard to see the curvature of RPE from the slow scan cross-sectional image of raster scan.

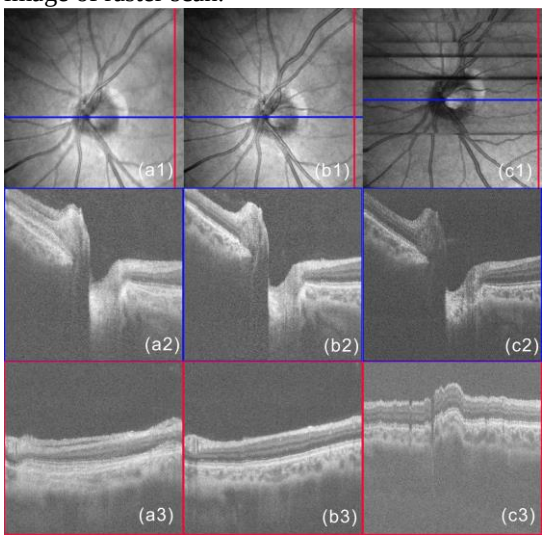

Figure 5. ONH images scanned with Lissajous and raster scan. Each column from left side represent remapped image of Lissajous scanned data (a) without and (b) with motion

correction, and (c) raster scanned image. Each row from upper side represent (1) *en face* projection, (2)horizontal or fast scan cross-section, and (3)vertical or slow scan cross-sections images.

REFERENCES

① W. Drexler and J. G. Fujimoto., "State-of-the-art retinal optical coherence tomography," Prog. Retin. Eye Res. 27(1), 2008, 45-88.

② Vienola K V, Braaf B, Sheehy C K, et al., "Real-time eye motion compensation for OCT imaging with tracking SLO," Biomed. Opt. Express 3(11), 2012, 2950-2963.

③ Kraus M F, Potsaid B, Mayer M A, et al., "Motion correction in optical coherence tomography volumes on a per A-scan basis using orthogonal scan patterns," Biomed. Opt. Express 3(6), 2012, 1182-1199.

④ Kraus M F, Liu J J, Schottenhamml J, et al., "Quantitative 3D-OCT motion correction with tilt and illumination correction, robust similarity measure and regularization," Biomed. Opt. Express 5(8), 2014, 2591-2613.

⑤ Hendargo H C, Estrada R, Chiu S J, et al., "Automated non-rigid registration and mosaicing for robust imaging of distinct retinal capillary beds using speckle variance optical coherence tomography," Biomed. Opt. Express 4(6), 2013, 803-821.

⑥ Bazaei A, Yong Y K, Moheimani S O R., "High-speed Lissajous-scan atomic force microscopy: Scan pattern planning and control design issues," Review of Scientific Instruments 83(6), 2012, 063701.

５．主な発表論文等
（研究代表者、研究分担者及び連携研究者には下線）

〔雑誌論文〕（計　5　件）

① Yiwei Chen, Young-Joo Hong, Shuichi Makita, and Yoshiaki Yasuno, “Three-dimensional eye motion correction by Lissajous scan optical coherence tomography,” *Biomed. Opt. Express* 8(3), Peer reviewed, 2017, 1783-1802. DOI: 10.1364/BOE.8.001783

② Young-Joo Hong, Yiwei Chen, En Li, Masahio Miura, Shuichi Makita and Yasuno Yoshiaki, “Eye motion corrected OCT imaging with Lissajous scan pattern,” *SPIE proceedings* 9693, 2016, 96930P. DOI: 10.1117/12.221227

③ Shuichi Makita, Kazuhiro Kurokawa, Young-Joo Hong, Masahiro Miura, Yoshiaki Yasuno, “Noise-immune complex correlation for optical coherence angiography based on standard and Jones matrix optical coherence tomography,” *Biomed. Opt. Express* 7(4), Peer reviewed, 2016, 1525-1548. DOI: 10.1364/BOE.7.001525

④ Satoshi Sugiyama, Young-Joo Hong, Deep Kasaragod, Shuichi Makita, Sato Uematsu, Yasushi Ikuno, Masahiro Miura, and Yoshiaki Yasuno, “Birefringence imaging of posterior eye by multi-functional Jones matrix opical coherence tomography,” *Biomed. Opt. Express* 6(12), Peer reviewed, 2015, 4951-4974. DOI: 10.1364/BOE.6.004951

⑤ Kazuhiro Kurokawa, Shuichi Makita, Young-Joo Hong, and Yoshiaki Yasuno, “In-plane and out-of-plane tissue micro-displacement measurement by correlation coefficients of optical coherence tomography,” *Optics Letters* 40(9), Peer reviewed, 2015, 2153-2156. DOI: 10.1364/OL.40.002153

〔学会発表〕（計　3　件）

① Young-Joo Hong, Yiwei Chen, En Li, Masahiro Miura, Shuichi Makita, Yoshiaki Yasuno, “Eye motion corrected OCT imaging with Lissajous scan pattern,” Photonis West, BiOS 2016.02.13, USA, San Francisco.

② Young-Joo Hong, Shuichi Makita, Masahiro Miura, Yoshiaki Yasuno, “Lissajous scan applied eye motion correction for OCT volume imaging,” Optics and Photonics Japan 2015.10.29, Japan, Tokyo.

③ Young-Joo Hong, Masahiro, Shuichi Makita Deepa Kasaragod, Satoshi Sugiyama, Yoshiaki Yasuno, “Mutifunctional OCT imaging of macular degeneration for vasculature, RPE, and choroid investigation,” ARVO 2015.05.06, USA, Denver.

〔図書〕（計　0　件）

〔産業財産権〕

○出願状況（計　0 件）

名称：
発明者：
権利者：
種類：
番号：
出願年月日：
国内外の別：

○取得状況（計　0　件）

名称：
発明者：
権利者：
種類：

番号：
取得年月日：
国内外の別：

〔その他〕
ホームページ等

６．研究組織
(1)研究代表者
洪 暎周（Hong, Young-Joo）
筑波大学・医学医療系・助教
研究者番号：40738431

(2)研究分担者
（　　）

研究者番号：

(3)連携研究者
（　　）

研究者番号：

(4)研究協力者
（　　）